

Phenotypic response of the diatom *Phaeodactylum tricornutum* Bohlin to experimental changes in the inorganic carbon system

Ana Bartual*, J. Angel Gálvez and Fernando Ojeda

Departamento de Biología, Facultad de Ciencias del Mar y Ambientales, Universidad de Cádiz, CASEM, Campus Río San Pedro, 11510-Puerto Real, Cádiz, Spain, e-mail: ana.bartual@uca.es

* Corresponding author

Abstract

The physiology and biochemistry of *Phaeodactylum tricornutum* have been extensively studied, and some aspects of its biology are well known. Phenotypic plasticity is probably one of its most remarkable features. Two basic morphotypes, fusiform and triradiate, can be found in natural liquid environments. Although the transformation from one morphotype to the other has been previously reported, ecological causes and consequences of such transformation remain unknown. Here, we report changes in the relative abundance of the two morphotypes of *Phaeodactylum* associated with changes in the inorganic carbon system. The relative abundance of the triradiate morphotype increased in cultures grown at either high pH or high dissolved inorganic carbon, and markedly so under subsaturating illumination for growth. At high pH, this increase was strongly correlated with a decrease in the overall culture growth rate. At the individual (cell) level, there was a larger increase in the surface area of the triradiate morphotype (resulting in a higher surface-to-volume ratio) than in the fusiform morph under subsaturating illumination for growth. These results provide new insights into the biology of this diatom, mainly related to the performance (fitness) of the two basic morphotypes under contrasting illumination for growth and different inorganic carbon conditions.

Keywords: cell morphology; CO₂; diatom ecology; dissolved inorganic carbon (DIC); phenotypic plasticity.

Introduction

Morphological alterations in microalgae are associated with changes in physiological and/or ecological parameters. In marine diatoms, changes in cell volume and surface-to-volume ratios driven by alterations in cell size or shape are associated with changes in photosynthesis, metabolic rates, nutrient uptake dynamics and, ultimately, growth rates (Taguchi 1976, Pahlow et al. 1997, Montagnes and Franklin 2001, Snoeijs et al. 2002, Sarthou et

al. 2005). Nevertheless, an analytical study of the functional responses of the different morphs to environmental parameters is required to shed light on the causal mechanisms driving such morphological variation. In this context, the marine diatom *Phaeodactylum tricornutum* Bohlin (Bacillariophyceae) constitutes an ideal model for study in that it has a marked polymorphism and significant morphological changes occur over short time scales (Wilson 1946, Borowitzka and Volcani 1978).

Phaeodactylum tricornutum is a rather atypical diatom species in the sense that individual cells are only partially silicified (Lewin et al. 1958, Borowitzka and Volcani 1978, Johansen 1991), and only oval cells are able to synthesize true silica valves (Borowitzka and Volcani 1978). However, an 18S rRNA phylogeny unmistakably places *P. tricornutum* (hereafter *Phaeodactylum*) within the pennate diatom lineage (Medlin et al. 2000, Medlin 2004). *Phaeodactylum* has been one of the most widely studied diatoms in the last 50 years and its genome has been sequenced recently (Monstant et al. 2005).

The species has two basic morphotypes in agitated liquid media, viz., triradiate and fusiform. The triradiate form may have equal or unequal arm lengths, the latter being associated with transitional stages between two basic morphotypes (Wilson 1946, Borowitzka and Volcani 1978). A distinct oval morphotype has also been described and this occurs with highest frequency on either solid media or in unagitated liquid cultures (Lewin et al. 1958, Gutenbrunner et al. 1994). Very recently, a new round morphotype associated with oval cell aggregates and stress conditions has been described (De Martino et al. 2007). Different environmental factors, such as light, UV radiation, nutrient availability, aeration, and temperature, have been reported as related to changes in the relative abundance of these morphotypes, both in controlled cultures and natural populations (Darley 1968, Behrenfeld et al. 1992).

We analyzed the response of a strain of *Phaeodactylum* with an initial 50:50 ratio of triradiate and fusiform morphotypes to alterations in the carbon dioxide availability in natural sea water under saturating- and subsaturating-light conditions. Specifically, we have implemented an experimental design aimed to test the existence of changes in (1) the relative abundance of *Phaeodactylum* morphotypes at the population (culture sample) level; and (2) morphometrical parameters – namely surface area, volume and surface-to-volume ratio – at the individual (cell) level associated with changes in pH and dissolved inorganic carbon (DIC) under two contrasting light intensities. Since both pH and DIC are critical parameters in the seawater carbon system (Skirrow 1965), this study provides novel insight into the relative perform-

ance of the two basic morphotypes of *Phaeodactylum* across different levels of carbon-dioxide availability.

Materials and methods

Phaeodactylum strain and culture conditions

The strain CCAP 1052/1A of *Phaeodactylum* obtained from the Alfred Wegener Institute culture collection was maintained in stock culture in filtered (0.2 μm) Atlantic seawater from the Gulf of Cádiz (southern Spain) under saturating and continuous white light [Sylvania (Danvers, MA, USA) GRO-LUX F36W-GRO T8] at pH 8.2 and constant temperature ($17.5 \pm 0.5^\circ\text{C}$). The two basic morphotypes and intermediate morphs were present in this stock culture: triradiate cells with equal (I) or unequal arms (II), and fusiform cells, either straight (III) or curved (also boomerang) (IV) (see Figure 1). The relative abundance of the two basic morphotypes was 50% (mean \pm SD: $48.7 \pm 4.9\%$ fusiform and $51.3 \pm 5.0\%$ triradiate). The stock was re-inoculated weekly and the relative abundance of the two morphotypes under the above-mentioned culture conditions remained stable at a 50:50 ratio throughout the experimental period (several months).

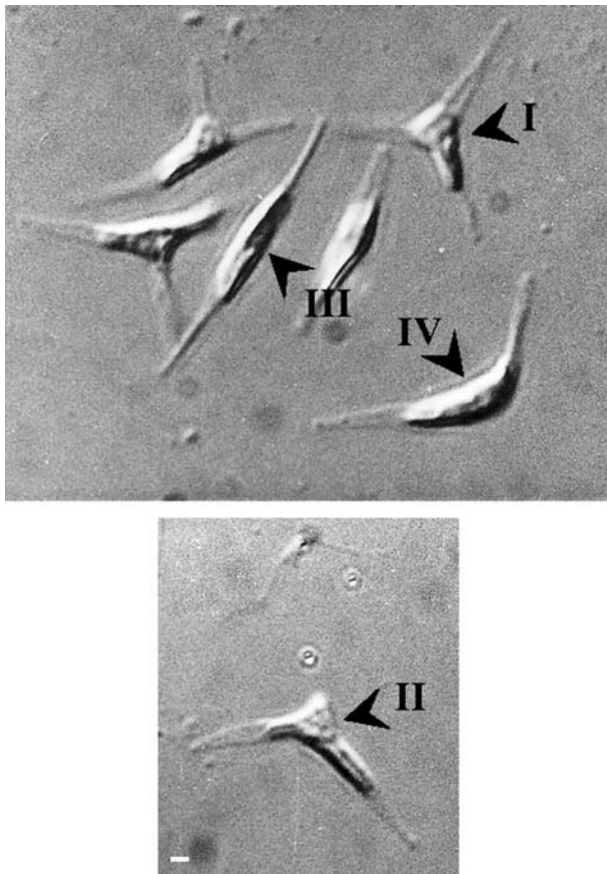


Figure 1 *Phaeodactylum tricornutum*: light micrographs showing different morphotypes (strain CCAP 1052/1A). Triradiate cells with equal arms (I), triradiate cells with unequal arms (II), fusiform cells (III), and boomerang fusiform cell (IV). Scale bar: 1 μm . Nomenclature of different morphotypes follows Wilson (1946) and Borowitzka and Volcani (1978).

Experimental design

Experimental cultures were grown in sterilized 1.2-l borosilicate glass bottles using natural, filtered (0.2 μm) Atlantic seawater (Gulf of Cádiz, Spain), enriched with f/2 medium (Guillard and Ryther 1962). Unbuffered culture media were used, since the use of buffers has been shown to affect the physiology of *Phaeodactylum* (Fábregas et al. 1993).

Experimental treatments were set by combinations of different pH values and different levels of DIC in saturating and subsaturating illumination for growth (150 and 30 $\mu\text{mol photons m}^{-2} \text{ s}^{-1}$) (Beardall and Morris 1976) on 14:10 light/dark (LD) cycles. Table 1 summarizes the different treatment levels and their chemical properties on day 0 (outset). For a detailed description of media preparation and analyses of their chemical properties, see Bartual and Gálvez (2002). Average temperature was $17.5 \pm 0.5^\circ\text{C}$ during the light phase and $15.5 \pm 0.5^\circ\text{C}$ during the dark phase. A total of 15 replicate bottles were used for each treatment level. Each bottle was inoculated with an identical low cell density (300–400 cell ml^{-1} at day 0) to ensure acclimation of the cells to the different inorganic carbon conditions, but preventing a strong alteration of the carbon system, which is affected by cell growth in unbuffered media. pH was used as a surrogate parameter for monitoring carbon system conditions, since slight changes from the pre-established pH in the cultures would be indicative of strong changes in the desired carbon conditions. As an example, an increase of 0.1 units of pH implies a decrease of $[\text{CO}_2(\text{aq})]$ from 12.5 to 9.4 μM for a seawater of 38 psu, 2.2 mM of DIC, pH 8.2 and 17.5°C . Therefore, one of the 15 bottles (reference bottle) was used for continually monitoring pH with a CRISON-2002 pH-meter (Crison Instruments S.A., Alella, Spain) using a combined AgCl/KCl glass electrode (CRISON 50-02) calibrated with National Bureau of Standards (NBS, Metrohm) buffer solutions.

Cells had been previously acclimated to the different experimental conditions for at least eight cell divisions (4–6 days). After inoculation, experimental bottles were closed without any headspace to avoid alteration of the pre-established pH and $[\text{CO}_2(\text{aq})]$ as a consequence of $\text{CO}_2(\text{g})$ diffusion. Every bottle was inverted three times a day during the light phase throughout the experiment in order to keep cells in suspension and avoid the transformation of cells into the oval morphotype, which is favored by unagitated conditions.

The experiment lasted 7 days for each treatment. Two bottles per treatment level were withdrawn randomly every day for cell counting, morphotype distinction, morphometric measurements of cells and determination of the carbon system. From each bottle, two 125-ml replicate samples were collected, fixed with Lugol's solution, and kept in cold, dark conditions until analysis. Withdrawn bottles were not further incubated.

Cell counting and relative abundance of morphotypes

Counting of cells and calculation of the relative abundance of the two basic morphotypes was carried out in the 125-ml Lugol's fixed samples by using the Utermöhl

Table 1 Summary of the chemical characteristics of experimental treatments.

Treatments	pH	TA ($\mu\text{eq l}^{-1}$)	[CO ₂ (aq)] (μM)	DIC (mM)
Saturating light (150 $\mu\text{mol photons m}^{-2} \text{s}^{-1}$)				
pH 7.9–Natural DIC	7.96 (17.2)	2387.3 \pm 4.42	24.8 \pm 0.6	2.20 \pm 0.03
pH 8.2–Natural DIC	8.19 (17.5)	2590.6 \pm 12.63	13.8 \pm 0.1	2.20 \pm 0.01
pH 8.9–Natural DIC	8.89 (17.5)	3366.9 \pm 71.76	2.0 \pm 0.0	2.22 \pm 0.01
pH 8.2–High DIC	8.19 (18.6)	4220.9 \pm 1.05	23.3 \pm 1.2	3.75 \pm 0.15
pH 8.2–Natural DIC	8.19 (17.5)	2590.6 \pm 12.63	13.8 \pm 0.1	2.20 \pm 0.01
pH 8.2–Low DIC ₁	8.19 (17.5)	1344.9	7.1	1.14
Subsaturating light (30 $\mu\text{mol photons m}^{-2} \text{s}^{-1}$)				
pH 7.9–Natural DIC	7.91 (17.8)	2233 \pm 56.41	22.5 \pm 0.9	2.07 \pm 0.01
pH 8.2–Natural DIC	8.19 (17.5)	2244.1 \pm 13.34	11.4 \pm 0.9	1.94 \pm 0.01
pH 8.9–Natural DIC	8.88 (17.7)	3331.2 \pm 23.76	2.2 \pm 0.1	2.25 \pm 0.01
pH 9.5–Natural DIC	9.50 (17.4)	3845.1 \pm 137.4	0.2 \pm 0.0	2.00 \pm 0.00
pH 8.2–High DIC	8.20 (18.7)	4075.5 \pm 2.12	21.7	3.70 \pm 0.03
pH 8.2–Natural DIC	8.19 (17.5)	2244.1 \pm 13.34	11.4 \pm 0.9	1.94 \pm 0.01
pH 8.2–Low DIC ₁	8.20 (17.6)	1686.1 \pm 9.33	9.4 \pm 1.0	1.52 \pm 0.02
pH 8.2–Low DIC ₂	8.19 (17.2)	521.16 \pm 8.69	2.9 \pm 0.4	0.38 \pm 0.01

Values are means \pm SD of four culture replicates. When SD is not given, there was no replication. Temperature for pH measurements is indicated in parentheses. pH was decreased or increased by adding 1 N solutions of HCl or NaOH, respectively. High DIC media were prepared by adding NaHCO₃ to natural seawater. Low DIC media were prepared by bubbling acidified seawater with CO₂-free air and adjusting the final pH to 8.2 by adding NaOH. See Bartual and Gálvez (2002) for further details of media preparation.

TA: total alkalinity, DIC: dissolved inorganic carbon.

inverted microscope technique (Utermöhl 1958) within 72 h of fixation. A minimum number of 400 cells per replicate were counted in order to keep the counting error within $\pm 10\%$ (Lund et al. 1958). Growth rates (μ) were then calculated as the slope of the linear regression of the total cell density (fusiform plus triradiate, log-transformed) against time. Since the proportion of the two basic morphotypes was not affected by culture age under either saturating or subsaturating light conditions (A. Bartual, unpublished data), a comparison of the relative abundance of the two morphotypes among treatments was made within the exponential growth phase, which corresponded to the average abundance value after 4 and 6 days of incubation in saturating and subsaturating light conditions, respectively.

Since cultures were not axenic, the presence of bacteria was checked in subsamples obtained from the cultures, preserved in 0.6% glutaraldehyde and stored in cold (4°C) dark conditions. Bacterial biomass was estimated using epifluorescence microscopy with 4',6-diamidino-2-phenylindole (DAPI) as the fluorochrome (Porter and Feig 1980), and it was found to be less than 10% of phytoplankton biomass in all instances.

Cell morphometry

Individual cell images were captured using an inverted microscope (Leitz, Fluovolt, Wetzlar, Germany) connected to a video camera CCD (Kappa, CF15/2, Gleichen, Germany) that allowed the analysis of cell morphology in a high resolution monitor (Mitsubishi, Tokyo, Japan). Subsequently, an image analysis program (VIDS-V, Analytical Instruments, Pampisford, Cambridge, UK) was used to obtain linear dimensions, which served for subsequent estimations of the volume and surface area of individual cells. Cell length was obtained in fusiform cells (*Hf*), and arm length for the three arms (*H_itr*; where $i=\{1, 2, 3\}$) in triradiate forms. Likewise, cell width was

obtained in fusiform cells (*Df*), and arm width of the three arms (*D_itr*; where $i=\{1, 2, 3\}$) in triradiate cells (see Figure 2). Cell volume and surface area were then calculated as indicated in Figure 2. Fusiform cells were assumed to be prolate spheroids (see Figure 2), an assumption applied to other diatoms of similar morphology (Hillebrand et al. 1999, Leynaert et al. 2004). In the case of triradiate cells, an ensemble of two prolate spheroids was needed to estimate volume and surface area (see Figure 2 for detailed explanation). Since the error coefficient of cell volume was found to stabilize for sample sizes larger than 60 in both morphotypes, 100 haphazardly selected cells of each morphotype were measured within each 125-ml sample.

Statistical analyses

To detect significant changes in the abundance of the two morphotypes, the relative abundance of the triradiate morphotype was used as the response variable and compared among different combinations of pH and DIC in the two saturating and subsaturating light conditions within the exponential growth phase (see above).

A two-way analysis of variance (ANOVA) was performed to test for differences in the relative abundance of the triradiate morphotype across treatments. In the first two-way ANOVA, the variables pH (7.9, 8.2, and 8.9; keeping DIC levels constant) and light intensity (subsaturating and saturating) were considered as fixed effects. In the second ANOVA, DIC treatment (high, natural, and low DIC₁) and light intensity were considered as fixed effects. Since a further higher level of pH (9.5) and a further lower level of DIC (low DIC₂) were considered under subsaturating light (but not under saturating light intensity, see Table 1), we tested for differences in the relative abundance of the triradiate morphotype across the whole range of pH and DIC levels under subsaturating light by

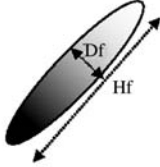
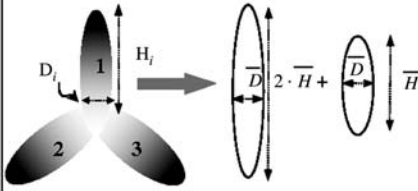
Morphotype	Volume and surface equation for geometric equivalent figure
Fusiform	
	$V_T = \text{cell volume}$ $V_T = \frac{\pi}{6} \cdot D_f^2 \cdot H_f$ $S_T = \text{cell surface}$ $S_T = \frac{\pi}{2} \cdot D_f \cdot \left(\frac{H_f}{e}\right) \cdot \text{sen}^{-1}\left(\frac{e}{H_f}\right)$
Triradiate	
 <p>$\bar{D}_{tr} = \text{mean}(D_i); i=1,2 \text{ and } 3$ $\bar{H}_{tr} = \text{mean}(H_i); i=1,2 \text{ and } 3$</p>	$V_T = \text{cell volume}$ $V_T = V + 0.5 \cdot V$ <i>being</i> $V = \frac{\pi}{6} \cdot \bar{D}_{tr}^2 \cdot 2 \cdot \bar{H}_{tr}$ $S_T = \text{cell surface}$ $S_T = S + 0.5 \cdot S$ <i>being</i> $S = \frac{\pi}{2} \cdot \bar{D}_{tr} \cdot \left(\frac{\bar{H}_{tr}}{e}\right) \cdot \text{sen}^{-1}\left(\frac{e}{\bar{H}_{tr}}\right)$ $e = \text{elipticity} = \frac{\sqrt{H^2 - D^2}}{H}$

Figure 2 *Phaeodactylum tricornutum*: geometric models and equations used for calculating cell volume and cell surface for two morphotypes.

Abbreviations: D =diameter, H =length, “ f ” denotes fusiform morphology, and “ t ” denotes triradiate form. Volume and surface in fusiform cells were calculated as a prolate spheroid of height “ H_f ” and diameter “ D_f ”. In triradiate cells, the summation of two prolate spheroids (the first of height “ $2H_{tr}$ ” and diameter “ D_{tr} ”, and the second of height “ H_{tr} ” and diameter “ D_{tr} ”) were considered for cell volume and cell surface calculations.

means of a one-way ANOVA and subsequent post-hoc Scheffé’s tests.

Differences in the overall growth rate [i.e., μ (triradiate plus fusiform)] between treatment levels were tested by means of analysis of covariance (ANCOVA) tests of homogeneity of slopes (Zar 1984). A first ANCOVA was applied to compare the overall growth rate between saturated and subsaturated light conditions under natural seawater pH and natural DIC level. Then, two separate (independent) ANCOVAs were implemented under each light condition to search for differences in growth rate across pH and DIC levels. When significant differences were detected, post-hoc planned comparisons (Dunnett’s tests; Zar 1984) were made between the growth rates under natural pH and natural DIC level (assumed as control) and each of the other treatment levels. Finally, the relationship between changes in the overall growth rate under all experimental conditions (only under subsaturating light) and the relative abundance of the tri-

radiate morphotype was explored by means of linear regression analysis.

Two further sets of two-way ANOVAs were also performed to search for differences in three cell morphometrical parameters (cell surface, cell volume, and surface-to-volume ratio) between morphotypes across pH and DIC levels within each light condition. In the first set, pH treatment (7.9, 8.2, and 8.9, DIC levels kept constant) and morphotype were considered as fixed effects in the ANOVA model. In the second set, DIC treatment (high, natural, and low DIC₁) and morphotype were considered as fixed effects. Since a further higher level of pH (9.5) and a further lower level of DIC (low DIC₂) were tested under subsaturating light (but not under saturating light conditions, see Table 1), we tested for the existence of differences in cell morphometry within each morphotype across the whole range of pH and DIC levels under subsaturating light by means of one-way ANOVAs and subsequent post-hoc Scheffé’s tests.

All data were checked for normality and homogeneity of variances prior to analysis (Zar 1984), and no transformations were needed.

Results

Relative abundance of morphotypes and culture growth rates

Experimental changes in the carbon system (either by changes of culture pH or DIC; see Table 1) clearly affected the relative abundance of the triradiate morphotype in the cultures. The effect of changes in the pH, keeping DIC constant at natural levels, depended on the level of light (saturating vs. subsaturating), as indicated by the significant pH×light interaction (Table 2). Whereas the relative abundance of the triradiate morphotype was slightly lower at a pH below natural seawater pH (i.e., 7.9) under subsaturating light, the effect was reversed at a pH value of 8.9, which is above natural seawater pH (Figure 3A). This trend of higher relative abundance of the triradiate morphotype with increasing pH levels and subsaturating light was further confirmed by the significant one-way ANOVA ($F_{3,24}=55.8$, $p<0.0001$; Figure 3A).

Changes in DIC levels at constant pH (8.2) also affected the relative abundance of the triradiate morphotype (Table 3) but did so in a bimodal manner (Figure 3B). The relative abundance of the triradiate morphotype was higher at either higher or lower DIC levels than at natural DIC levels. This pattern was more conspicuous under subsaturating light and was reaffirmed by the significant one-way ANOVA ($F_{3,16}=98.1$, $p<0.0001$) when an even lower DIC level (low DIC₂) was considered (see Figure 3B).

Growth rate in cultures at natural seawater pH and natural DIC levels under subsaturating light conditions was significantly lower ($F_{1,15}=93.8$, $p<0.0001$; homogeneity of slopes ANCOVA) than under saturating light conditions. While growth rate was similar ($F_{4,42}=0.26$, $p=0.9$; homogeneity of slopes ANCOVA) across pH and treatment levels under saturating light conditions, significant differences were detected under subsaturating light ($F_{6,36}=2.58$, $p=0.035$; homogeneity of slopes ANCOVA). Growth rate seemed limited under subsaturating light in all conditions assayed, but particularly so at higher pH or lower DIC levels (Table 4).

When pooling all pH/DIC treatments, average growth rates under subsaturating light conditions were inversely correlated with relative abundance of the triradiate morphotype (Figure 4).

Cell morphometry

Average cell volumes, surface areas, and surface-to-volume ratios of each morphotype within the exponential growth phase under all experimental conditions are shown in Figures 5 and 6. Keeping DIC constant at natural levels, average cell surface and cell volume were significantly higher in the triradiate morphotype across all pH treatments under saturating light. Both morphometrical parameters increased with increasing pH in a similar way in the two morphotypes, as indicated by the lack of significant interaction between pH and morphotype

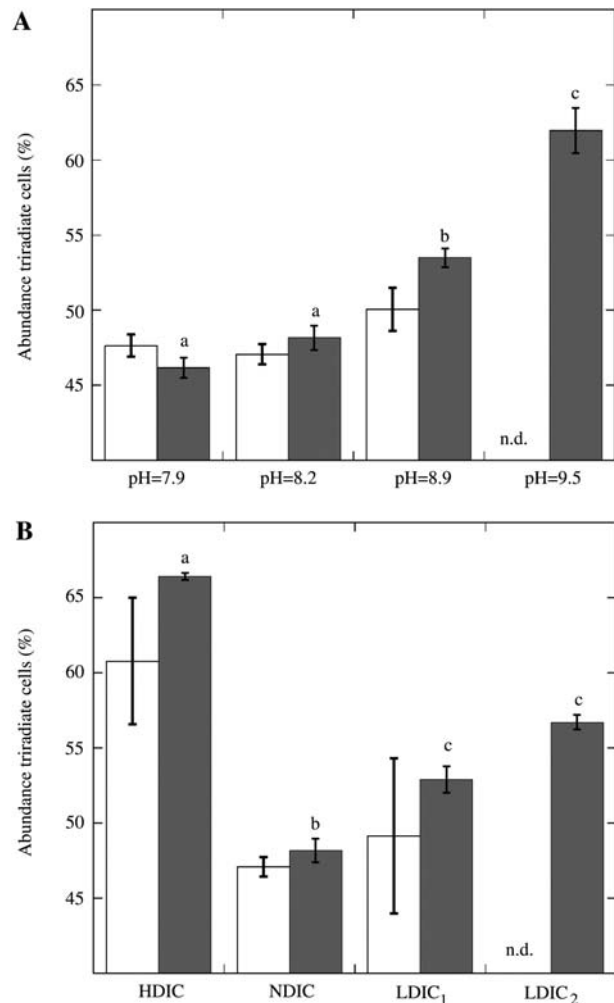


Figure 3 *Phaeodactylum tricorutum*: average relative abundance of the triradiate morphotype in exponentially growing cultures under saturating (white bars) and subsaturating (shaded bars) light conditions at different pH (A) and DIC (B) levels. Different letters indicate significant pairwise differences between treatments (Scheffé's test, $\alpha=0.05$) after the one-way ANOVA under subsaturating light. HDIC, high DIC; NDIC, natural DIC; LDIC₁, low DIC₁; LDIC₂, low DIC₂ (see materials and methods section for details).

Table 2 *Phaeodactylum tricorutum*: two-way ANOVA of the effects of pH and light conditions on the relative abundance (%) of the triradiate morphotype.

Source of variation	df	MS	F	p
pH	2	79.0	19.1	<0.001
Light	1	9.9	2.4	0.131
pH×light	2	17.2	4.2	0.024
Error	35	4.1		

Table 3 *Phaeodactylum tricorutum*: two-way ANOVA of the effects of dissolved inorganic carbon (DIC) levels and light conditions on the relative abundance (%) of the triradiate morphotype.

Source of variation	df	MS	F	p
DIC	2	740.5	38.7	<0.001
Light	1	76.0	4.0	0.057
DIC×light	2	15.4	0.8	0.458
Error	25	19.1		

Table 4 *Phaeodactylum tricornutum*: growth rates (μ , day⁻¹) under different light, pH, and dissolved inorganic carbon (DIC) conditions.

Treatment	Saturating light (150 $\mu\text{mol photons m}^{-2} \text{s}^{-1}$)	Subsaturating light (30 $\mu\text{mol photons m}^{-2} \text{s}^{-1}$)
pH 7.9–Natural DIC	1.37 (± 0.001)	0.91 (± 0.042)
pH 8.2–Natural DIC	1.29 (± 0.049)	0.97 (± 0.021)
pH 8.9–Natural DIC	1.25 (± 0.051)	0.73 (± 0.017)
pH 9.5–Natural DIC	ND	0.68 (± 0.020)*
pH 8.2–High DIC	1.39 (± 0.035)	0.88 (± 0.064)
pH 8.2–Low DIC ₁	1.29 (± 0.049)	0.71
pH 8.2–Low DIC ₂	ND	0.61*

Values are means (\pm SD). * Indicates significant differences ($\alpha=0.05$) after post-hoc planned comparisons (Dunnnett's test) between each treatment level and the pH 8.2–natural DIC treatment (considered as a control). ND, no data.

effects (Table 5; Figure 5A,B). By contrast, no significant differences in surface-to-volume ratio were found between morphotypes (Table 5), and this parameter decreased with increasing pH (Figure 5C) in similar ways for both morphotypes (no significant pH \times morphotype interaction; see Table 5). Under subsaturating light intensity, average cell surface and cell volume were consistently significantly higher in the triradiate morphotype across all pH treatments (Table 5; Figure 5D,E). However, under such limiting light conditions, the response of the two morphotypes to increasing pH was markedly different, especially for cell surface (Figure 5D; pH \times morphotype interaction: $p=0.035$), and less so for cell volume (Figure 5E; pH \times morphotype interaction: $p=0.058$). A further analysis excluding cell surface values for pH=9.5, which were not analyzed for saturating light, showed an even more significant pH \times morphotype interaction ($p=0.013$). Under subsaturating light, surface-to-volume ratio was consistently higher in the triradiate morphotype across all pH levels (Figure 5F), and both morphotypes responded to the pH effect in similar ways (no significant pH \times morphotype interaction; see Table 5).

Average cell surface and, to a less extent, cell volume were significantly higher in the triradiate morphotype under saturating light across all DIC treatments (Table 6; Figure 6A,B), reaching highest values at high DIC levels (Figure 6A,B). Both morphotypes were similarly affected

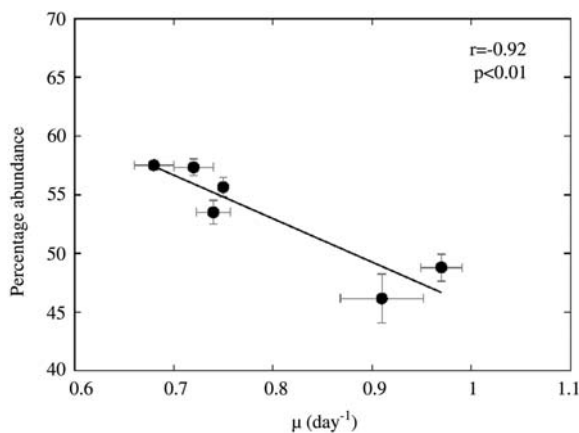


Figure 4 *Phaeodactylum tricornutum*: linear relationship between percentage abundance of the triradiate morphotype and growth rates under subsaturating light conditions and different inorganic carbon availabilities (see Table 1 for details). Values are means \pm SE.

by the DIC effect (no significant DIC \times morphotype interaction; Table 6). By contrast, the surface-to-volume ratio seemed to follow a similar, unimodal pattern of variation across DIC levels in the two morphotypes (Figure 6C; no significant DIC \times morphotype interaction; see Table 6). Under subsaturating light intensity, average cell surface was significantly higher in the triradiate morphotype (Table 6), particularly under the lowest DIC levels (low DIC₂; Figure 6D). Under such limiting light conditions, the responses of the two morphotypes to changes in DIC levels were markedly different for both cell surface

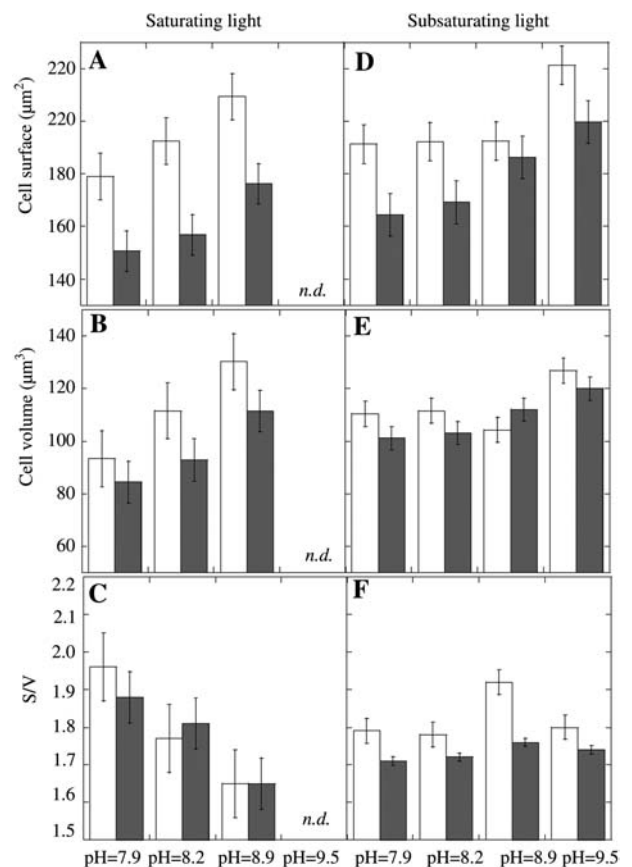


Figure 5 *Phaeodactylum tricornutum*: average cell surface (A,D), cell volume (B,E), and surface-to-volume ratio (C,F) of triradiate (white bars) and fusiform (dark bars) morphotypes grown at saturating (150 $\mu\text{mol photons m}^{-2} \text{s}^{-1}$) and subsaturating (30 $\mu\text{mol photons m}^{-2} \text{s}^{-1}$) light and different pH conditions (see Table 1 for details). Values are means \pm SE; $n=100$.

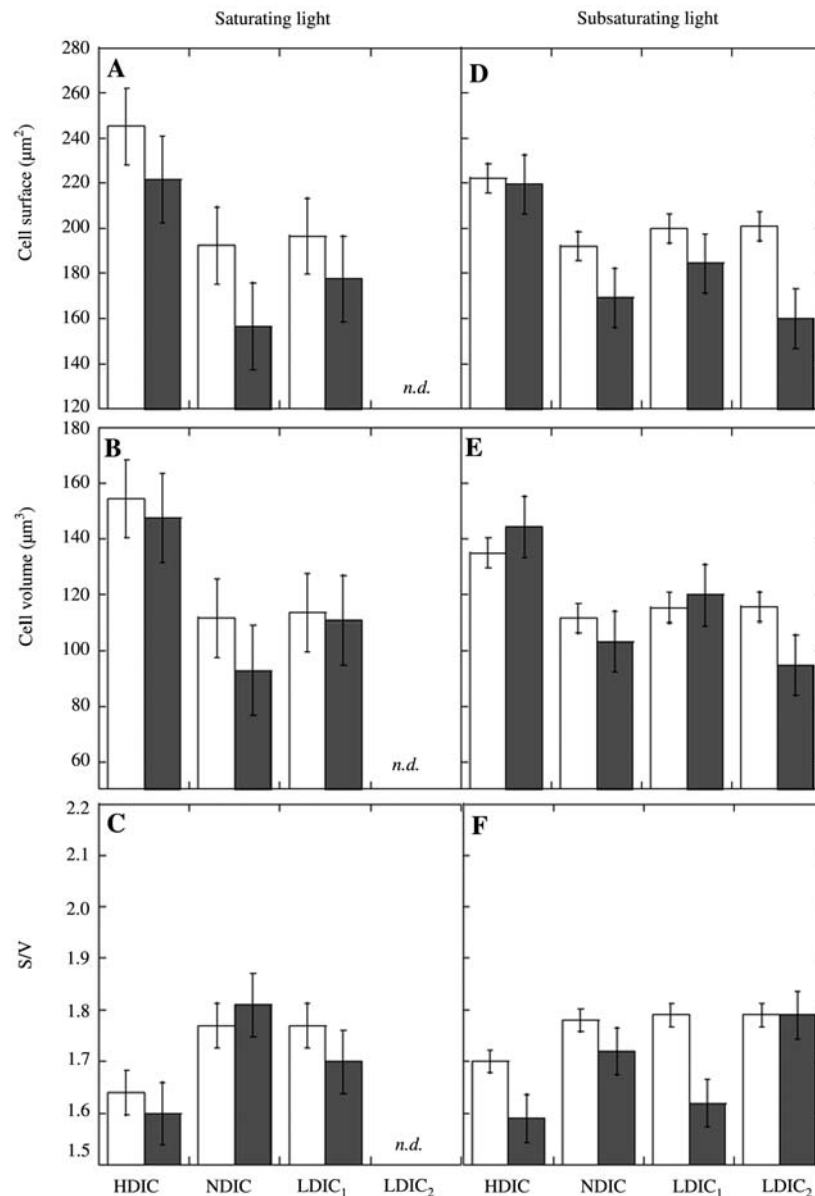


Figure 6 *Phaeodactylum tricornutum*: average cell surface (A,D), cell volume (B,E), and surface-to-volume ratio (C,F) of triradiate (white bars) and fusiform (dark bars) morphotypes grown at saturating ($150 \mu\text{mol photons m}^{-2} \text{s}^{-1}$) and subsaturating ($30 \mu\text{mol photons m}^{-2} \text{s}^{-1}$) light and different DIC conditions (see Table 1 for details). HDIC, high DIC; NDIC, natural DIC; LDIC₁, low DIC₁; LDIC₂, low DIC₂. Values are means \pm SE; $n=100$.

(DIC \times morphotype interaction: $p < 0.0001$) and cell volume (DIC \times morphotype interaction: $p < 0.0001$; see Table 6). These differences between morphotypes were due, to a large extent, to conspicuous differences in cell surface and cell volume at lowest DIC conditions (low DIC₂; see Figure 6D,E). Finally, under subsaturating light, surface-to-volume ratio was higher in the triradiate morphotype (Table 6), except under the lowest DIC level (low DIC₂; see Figure 6F), where differences seemed to vanish.

Discussion

Apart from *Phaeodactylum*, a triradiate form has been reported in other pennate diatom genera (e.g., Schmid 1997, Sabbe et al. 2004, Morales 2005). This triradiate form has been frequently described as an abnormal, ter-

atological form associated with environmental changes and without a truly adaptive value (but see Morales 2005). In this study, we report the existence of changes in the relative abundance of two basic morphotypes of *Phaeodactylum* (fusiform and triradiate) at the population (culture) level associated with experimental alterations in the carbon system. The novelty of our study is that we have been able to infer a plausible ecological advantage of the triradiate morphotype in experimental cultures under stressful conditions determined by subsaturating light and limiting carbon dioxide levels.

The increasing dominance of the triradiate morphotype (from an initial 50:50 ratio of triradiate and fusiform cells) at high pH and low DIC levels (i.e., low CO₂) under subsaturating light intensity may be a consequence of a comparatively superior ecological performance of the triradiate morphotype under stress conditions of low light

Table 5 *Phaeodactylum tricornutum*: two-way ANOVA of the effects of pH levels and morphotype (both fixed effects) on cell surface, cell volume, and S:V ratio under saturating and subsaturating light conditions.

Source of variation	Cell surface			Cell volume			S:V ratio					
	df	MS	F	p	df	MS	F	p	df	MS	F	p
Saturating light (150 $\mu\text{mol photons m}^{-2} \text{ s}^{-1}$)												
pH	2	39,796	34.69	<0.0001	2	49,253	45.94	<0.0001	2	3,681	52.31	<0.0001
Morphotype	1	152,346	133.05	<0.0001	1	35,667	33.27	<0.0001	1	0.031	0.44	0.5062
pH \times morphotype	2	647	0.55	<0.5786	2	1228	1.145	0.3189	2	0.135	1.91	0.1485
Error	571	1145			571	1072			571	0.070		
Subsaturating light (30 $\mu\text{mol photons m}^{-2} \text{ s}^{-1}$)												
pH	3	43,724	35.65	<0.0001	3	14,054	11.48	<0.0001	3	629,630	4.27	0.0005
Morphotype	1	78,247	63.80	<0.0001	1	4400	3.59	<0.0001	1	4,184,039	28.39	<0.0001
pH \times morphotype	3	3538	2.88	0.0348	3	2451	2.00	0.0583	3	176,338	1.19	0.2571
Error	794	1227			794	1224			794	147,336		

Table 6 *Phaeodactylum tricornutum*: two-way ANOVA of the effects of dissolved inorganic carbon (DIC) levels and morphotype (both fixed effects) on cell surface, cell volume, and S:V ratio under saturating and subsaturating light conditions.

Source of variation	Cell surface			Cell volume			S:V ratio					
	df	MS	F	p	df	MS	F	p	df	MS	F	p
Saturating light (150 $\mu\text{mol photons m}^{-2} \text{ s}^{-1}$)												
DIC	2	194,285	129.33	<0.0001	2	133,629	78.86	<0.0001	2	1,554	22.94	<0.0001
Morphotype	1	103,077	68.61	<0.0001	1	13,252	7.821	0.0053	1	0.083	1.23	0.2678
DIC \times morphotype	2	3847	2.56	0.0781	2	3457	2.04	0.1309	2	0.132	1.95	0.1430
Error	602	1052			602	1694			602	0.068		
Subsaturating light (30 $\mu\text{mol photons m}^{-2} \text{ s}^{-1}$)												
DIC	3	70,327	52.14	<0.0001	3	48,073	35.38	<0.0001	3	0.767	11.67	<0.0001
Morphotype	1	79,316	58.81	<0.0001	1	2630	1.94	0.1645	1	1.57	23.88	0.0001
DIC \times morphotype	3	11,814	8.76	<0.0001	3	8856	2.86	<0.0001	3	0.266	4.05	0.0072
Error	768	1349			768	1358			768	1349		

and CO₂. As previously reported (John-McKay and Colman 1997), and very recently corroborated (Szabo and Colman 2007), strain CCAP-1052/1A of *Phaeodactylum* lacks an external carbonic anhydrase enzyme (CA_{ext}, a zinc-containing enzyme that catalyzes the reversible transformation of bicarbonate into CO₂) and has only an internal CA (CA_{int}). The lack of CA_{ext} indicates that the major flux of DIC into the cells is in the form of HCO₃⁻, which implies an energy cost and a limitation of DIC uptake under subsaturating light conditions. At pH=9.5, most of the medium DIC is available as bicarbonate, and the low CO₂ available diffuses rapidly into the cell. Triradiate cells of *Phaeodactylum* under low light-high pH conditions had a larger surface area and higher surface-to-volume ratio than the fusiform morph. This could provide a physiological advantage under limiting light conditions by optimizing light capture and nutrient uptake efficiencies and increasing the surface of available membranes for enzymatic activity and/or molecular diffusion of inorganic carbon into the cell (Pahlow et al. 1997).

Since population changes in relative abundance of the two morphotypes are produced by and maintained across cell generations, it could be argued that both have an adaptive value in *Phaeodactylum tricornutum* and that relative fitness of the triradiate form would be higher than that of the fusiform under low light and limiting carbon availability. Nevertheless, when the medium was DIC-enriched, keeping a constant pH (8.2), the relative abundance of the triradiate morphotype was highest under both saturating and subsaturating light conditions (see Figure 3B). These results seem to contradict the otherwise steady patterns, since medium CO₂ is not limiting under high DIC (see Table 1), as can also be deduced from the culture growth rate values (Table 4). However, experimental DIC enrichment was achieved by adding NaHCO₃ to the culture medium (see Table 1). This also alters other chemical properties of the medium, such as the proportion of dissolved cations and osmolality. This osmotic alteration represents a different environmental stress condition and it is known to trigger rapid changes in cytosolic calcium concentrations in *Phaeodactylum* so as to re-establish osmotic and ion homeostasis (Falcitatore et al. 2000). At the longer time scale in which photosynthesis acts, there are other larger molecules, such as proline, that act as compatible solutes and could drive osmotic and homeostatic adjustments in *Phaeodactylum* (Schobert 1980, Schobert and Marsh 1982). The vacuole is the main organelle involved in osmotic and ionic homeostasis both by accumulation or mobilization of cations (e.g., Ca²⁺) and compatible solutes (e.g., proline). Interestingly, one of the most patent internal differences between morphotypes of *Phaeodactylum* is the vacuolar volume, which is considerably larger in triradiate cells (Borowitzka and Volcani 1978). Therefore, triradiate cells would also outperform fusiform cells under challenging osmotic conditions, such as those driven by the experimental DIC enrichment, owing to a likely more effective osmotic adjustment.

Associated with the increase in triradiate morphotype abundance, cell morphometry was also altered in response to changing pH, increasing cell volume and cell

surface area at high pH values in both morphotypes under saturating and subsaturating light conditions (see Figure 5). Long-term increase in phytoplankton cell volume is usually associated with a decrease in growth rate or with accumulation of storage compounds. The biochemical composition of *Phaeodactylum* adapted to subsaturating light and pH 9.5 (i.e., low CO₂) illustrated in a previous work (Bartual and Gálvez 2002) suggests the existence of lipid storage, which could account for this increase in cell volume under such limiting conditions. Cells of *Phaeodactylum* grown under these low light-low CO₂ conditions also showed a reduction in growth rate (Table 4). Under saturating light conditions, cell volume increased with increasing pH but, in this case, without a concomitant reduction in growth rate (see Table 4). According to Bartual and Gálvez (2002), the biochemical composition of *Phaeodactylum* cells grown under saturating light and high pH does not suggest the existence of storage.

Nevertheless, to accept unequivocally an increase of the triradiate form in cultures as the outcome of an adaptational advantage in this strain under stressful conditions (e.g., low light-limiting CO₂, osmotic stress), a higher fitness of the outperforming morphotype should be demonstrated. This requires an appropriate experimental approach specifically aimed to answer this crucial question. However, the reported increase in cell surface of the triradiate morphotype under limiting light conditions, resulting in a higher surface-to-volume ratio, is an appealing argument to suggest an ecological advantage for the triradiate form of *Phaeodactylum* over the fusiform under environmentally stressed conditions.

Considering that triradiate cells of *Phaeodactylum* spontaneously revert to fusiform across generations (Wilson 1946, Borowitzka and Volcani 1978, De Martino et al. 2007, A. Bartual, personal observations), an increase in the relative abundance of the triradiate morphotype in the experimental cultures may also be explained by a presumably lower transformation rate from triradiate to fusiform cells under certain conditions. However, preliminary results of an ongoing study have not detected any variation in the triradiate-to-fusiform transformation rate among experimental treatments (B. Villazán and A. Bartual, unpublished data).

Although this diatom species is not a typical component of the marine phytoplankton, *Phaeodactylum* has been used as a standard model for understanding diatom biology and its genome has recently been sequenced (Monstant et al. 2005). This provides an encouraging prospect for further studies of the biology of this diatom.

Acknowledgements

The authors thank the BIO II group from the Alfred Wegener Institute for providing us with *Phaeodactylum tricornutum*, clone CCAP 1052/1A. This work has been supported by a grant from Consejería de Educación y Ciencia de la Junta de Andalucía to A.B. and by a research grant attached to a "Ramón y Cajal" contract (MCYT-UCA) to F.O. We also thank Anthony R.O. Chapman and two anonymous reviewers for useful comments in a previous version of this manuscript.

References

- Bartual, A. and J.A. Gálvez. 2002. Growth and biochemical composition of the diatom *Phaeodactylum tricorutum* at different pH and inorganic carbon levels under saturating and subsaturating light regimes. *Bot. Mar.* 45: 491–501.
- Beardall, J. and I. Morris. 1976. The concept of light intensity adaptation in marine phytoplankton: some experiments with *Phaeodactylum tricorutum*. *Mar. Biol.* 37: 377–387.
- Behrenfeld, M.J., J.T. Hardy and H. Lee II. 1992. Chronic effects of ultraviolet-B radiation on growth and cell volume of *Phaeodactylum tricorutum* (Bacillariophyceae). *J. Phycol.* 28: 757–760.
- Borowitzka, M.A. and B.E. Volcani. 1978. The polymorphic diatom *Phaeodactylum tricorutum*: ultrastructure of its morphotypes. *J. Phycol.* 14: 10–21.
- Darley, W.M. 1968. Deoxyribonucleic acid content of the three cell types of *Phaeodactylum tricorutum* Bohlin. *J. Phycol.* 4: 219–220.
- De Martino, A., A. Meichenin, J.S. Kehou Pan and C. Bowler. 2007. Genetic and phenotypic characterization of *Phaeodactylum tricorutum* (Bacillariophyceae) accessions. *J. Phycol.* 43: 992–1009.
- Fábregas, J., V. Vázquez, B. Cabeza and A. Otero. 1993. Tris not only controls pH of microalgal culture but also feeds bacteria. *J. Appl. Phycol.* 5: 543–545.
- Falciatore, A., M. Ribera, D. Alcalá, P. Croot and C. Bowler. 2000. Perception of environmental signals by a marine diatom. *Science* 288: 2363–2366.
- Guillard, R.R. and J.H. Ryther. 1962. Studies on marine planktonic diatoms. *Can. J. Microbiol.* 8: 229–239.
- Gutenbrunner, S.A., J. Thalhamer and A.M. Schmid. 1994. Proteinaceous and immunochemical distinctions between the oval and fusiform morphotypes of *Phaeodactylum tricorutum* (Bacillariophyceae). *J. Phycol.* 30: 129–136.
- Hillebrand, H., C.D. Dürselen, D. Kirschtel, U. Pollinger, T. Zohary. 1999. Biovolume calculation for pelagic and benthic microalgae. *J. Phycol.* 35: 403–424.
- Johansen, J.R. 1991. Morphological variability and cell wall composition of *Phaeodactylum tricorutum* (Bacillariophyceae). *Great Bas. Nat.* 51: 310–315.
- John-McKay, M. and B. Colman. 1997. Variation in the occurrence of external carbonic anhydrase among strains of the marine diatom *Phaeodactylum tricorutum* (Bacillariophyceae). *J. Phycol.* 33: 988–990.
- Lewin, J.C., R.A. Lewin and D.E. Philpott. 1958. Observations on *Phaeodactylum tricorutum*. *J. Gen. Microbiol.* 18: 418–426.
- Leynaert, A., E. Bucciarelli, P. Claquin, R.C. Dugdale, V. Martin-Jézéquel, P. Pondaven and O. Ragueneau. 2004. Effect of iron deficiency on diatom cell size and silicic acid uptake kinetics. *Limnol. Oceanogr.* 49: 1134–1143.
- Lund, J.W.G., C. Kipling and D.E. LeCren. 1958. The inverted microscope method of estimating algal numbers and statistical basis of estimations by counting. *Hydrobiologia* 11: 143–170.
- Medlin, L.K. 2004. Evolution of the diatoms: V. Morphological and cytological support for the major clades and a taxonomic revision. *Phycologia* 43: 245–270.
- Medlin, L.K., W.C.H.F. Kooistra and A.M.M. Schmid. 2000. A review of the evolution of the diatoms: a total approach using molecules, morphology and geology. In: (A. Witkowski and J. Sieminska, eds.) *The origin and early evolution of the diatoms*. Polish Academy of Sciences, Krakow, Poland. pp. 13–35.
- Monstant, A., K. Jabbari, U. Matheswari and C. Bowler. 2005. Comparative genomics of the diatom *Phaeodactylum tricorutum*. *Plant Physiol.* 137: 500–513.
- Montagnes, D.J.S. and D.J. Franklin. 2001. Effect of temperature on diatom volume, growth rate, and carbon and nitrogen content: reconsidering some paradigms. *Limnol. Oceanogr.* 46: 2008–2018.
- Morales, E.A. 2005. Observations of the morphology of some known and new fragilarioid diatoms (Bacillariophyceae) from rivers in the USA. *Phycol. Res.* 53: 113–133.
- Pahlow, M., U. Riebesell and D. Wolf-Gladrow. 1997. The impact of cell shape and chain formation on nutrient acquisition of marine diatoms. *Limnol. Oceanogr.* 42: 1660–1672.
- Porter, K.G. and Y.S. Feig. 1980. The use of DAPI for identifying and counting aquatic micro flora. *Limnol. Oceanogr.* 25: 943–948.
- Sabbe, K., V.A. Chepurinov, W. Vyverman and D. Mann. 2004. Apomixis in *Achnanthes* (Bacillariophyceae); development of a model system for diatom reproductive biology. *Eur. J. Phycol.* 39: 327–341.
- Sarthou, G., K.R. Timmermans, S. Blain and P. Tréguer. 2005. Growth physiology and fate of diatoms in the ocean: a review. *J. Sea Res.* 53: 25–42.
- Schmid, A.M.M. 1997. Intracolonial variation of the tripolar pennate diatom *Centronella reiheltii* in culture: strategies of reversion to the bipolar *Fragilaria*-form. *Nova Hedwigia* 65: 27–45.
- Schobert, B. 1980. Proline catabolism, relaxation of osmotic strain and membrane permeability in the diatom *Phaeodactylum tricorutum*. *Physiol. Plantarum* 50: 37–42.
- Schobert, B. and D. Marsh. 1982. Spin label studies on osmotically-induced changes in the aqueous cytoplasm of *Phaeodactylum tricorutum*. *Biochim. Biophys. Acta* 720: 87–95.
- Skirrow, G. 1965. The dissolved gases – carbon dioxide. In: (J.P. Riley and G. Skirrow, eds.) *Chemical oceanography*. Vol. 1. Academic Press, London. pp. 163–196.
- Snoeijs, P., S. Busse and M. Potapova. 2002. The importance of diatom cell size in community analysis. *J. Phycol.* 38: 265–272.
- Szabo, E. and B. Colman. 2007. Isolation and characterization of carbonic anhydrases from the marine diatom *Phaeodactylum tricorutum*. *Physiol. Plant.* 129: 484–492.
- Taguchi, S. 1976. Relationship between photosynthesis and cell size of marine diatoms. *J. Phycol.* 12: 185–189.
- Utermöhl, H. 1958. Zur Vervollkommnung der quantitativen Phytoplankton-Methodik. *Mitteil. Int. Verein. Limnol.* 9: 1–38.
- Wilson, D.P. 1946. The triradiate and other forms of *Nitzschia closterium* (Ehrenberg) Wm. Smith, forma *minutissima* of Allen and Nelson. *J. Mar. Biol. Assoc. UK* 24: 235–270.
- Zar, J.H. 1984. *Biostatistical analysis*. 2nd edition. Prentice Hall, New Jersey, USA. 717 pp.

Received 18 September, 2007; accepted 20 June, 2008